ORIGINAL ARTICLE

In Silico and *in Vitro* Studies of Selected Citrus Plants on the Inhibition of Pancreatic Lipase

Khairul Niza Abdul Razak1, Syarifuddin Husain[1,2], Siti Zuraidah Mohamad Zobir[2], Adibah Amirah Abdul Nasir[1], Nur Najihah Ismail[3], Suriani Mohamad[1], Selestin Rathnasamy[1], Habibah A Wahab[1], *Ezatul Ezleen Kamarulzaman[1,2]

[1] School of Pharmaceutical Sciences, Universiti Sains Malaysia, 11800 Penang, Malaysia
[2] Malaysian Institute of Pharmaceuticals and Nutraceuticals, National Institutes of Biotechnology Malaysia, Halaman Bukit Gambir, 11700 Gelugor, Penang, Malaysia
[3] School of Biological Sciences, Universiti Sains Malaysia, 11800 Penang, Malaysia

ABSTRACT

Introduction: Obesity can lead to death with associated high-risk diseases such as cardiovascular disease, diabetes, hypertension, stroke and cancer. Obesity results from an excessive dietary fat intake. Pancreatic lipase (PL) is an enzyme that plays a major role in hydrolyzing fats into monoacylglycerol and fatty acids that can be absorbed into the small intestine. One of the strategies to treat obesity is by reducing fat absorption via PL inhibition. This study aims to search for potential PL inhibitors from selected Malaysian plants capable of reducing fat absorption. **Methods:** Potential PL inhibitors were virtually screened using AutoDock Vina against reported phytochemical compounds from the peels, fruits and leaves of five selected citrus plants namely *Citrus aurantifolia* (*C. aurantifolia*), *C. grandis*, *C. medica*, *C. hystrix* and *C. microcarpa*. **Results:** The results were classified based on the free energy of binding into three groups: high, moderate, and low inhibition. Eight compounds exhibited high activity against PL. Citrus grandis contributed the highest number of compounds, followed by *C. medica*, *C. microcarpa*, *C. aurantifolia*, and *C. hystrix*. To validate these findings, 15 methanolic extracts from various parts of these citrus plants were subjected to *in vitro* bioassays. Notably, the fruit extract of *C. medica* demonstrated the most potent PL inhibition at 62.59%, possibly due to the presence of diosmetin-6-C-glucoside. **Conclusions:** In conclusion, virtual screening of small molecules derived from selected citrus plants offers valuable insights into molecular docking and *C. medica* emerges as a potential anti-obesity plant.

Keywords: Pancreatic lipase; Anti-obesity; Orlistat; Citrus; Molecular docking

Corresponding Author:
Ezatul Ezleen Kamarulzaman, PhD
Email: ezatulezleen@usm.my
Tel: +604-6536667

INTRODUCTION

Obesity and excess weight have emerged as significant global health concerns. Malaysia is at an alarming rate of obesity being ranked as the most obese population in South-East Asian countries. In essence, obesity can be described as an outcome arising from an imbalance between calorie intake and expenditure by the body [1]. Another perspective defines obesity as a medical condition characterized by the excessive accumulation of body fat due to an energy imbalance [2]. Consequently, obesity is a complex condition that significantly elevates the risk of various serious metabolic disorders, including diabetes, hypertension, stroke, osteoarthritis, cancer, cardiovascular diseases, and sleep-breathing disorders [3].

A person is categorised as obese if the Body Mass Index (BMI) equals or exceeds 30 (30kg/m2) [4]. Obesity brings out various physical issues, including sleep apnea, joint pain, a shortened life expectancy, and a decline in overall quality of life [5-8]. Multiple approaches exist for addressing obesity, encompassing dietary therapy, physical activity, behavioural therapy, and pharmacotherapy [9-11]. In terms of pharmacotherapy, one strategy involves the prevention of obesity through the inhibition of pancreatic lipase activity, which, in turn, suppresses the digestion and absorption of dietary fat [12, 13].

Obesity treatment encompasses two mechanisms: one is centrally acting, which regulates food intake, while the other is peripherally acting, governing the absorption, storage, and metabolism of dietary fat [14-17]. Within our body, lipase, a pancreatic enzyme, plays a pivotal role in the digestion and absorption of dietary fats. In fact, pancreatic lipase is responsible for catalyzing 50% to 70% of the total dietary fats

hydrolysis [18]. Research has demonstrated that inhibiting pancreatic lipase (PL) can effectively reduce plasma triglyceride levels, thereby lowering the likelihood of obesity [19]. Orlistat is one of the drugs approved by the US Food and Drug Administration (US FDA) that works by suppressing the activity of the pancreatic lipase enzyme [20-22]. Nonetheless, orlistat can lead to significant adverse effects in patients, including steatorrhea, fecal incontinence and flatulence [18]. Moreover, orlistat also carries a potential risk of causing vitamin deficiencies and liver disorders.

Computational studies are becoming more widely embraced for their efficiency in saving time and reducing the financial and human resource demands in the drug discovery process. Their primary objective is to streamline the identification of potential drug candidates for specific target proteins. Computational methods have been instrumental in designing and exploring potential novel compounds to combat a range of diseases, proving both highly accurate and efficient in the process [23, 24]. Citrus plants have enjoyed a historical presence in Asian countries, not only as components of food and beverages but also as traditional herbal remedies. Kawaguchi et al. (1997) discovered that the fruit extracts of Citrus paradisi (C. paradisi) and C. limon demonstrated inhibition percentages of 55% and 49% against PL, respectively [19]. Additionally, hesperidin, isolated from the fruit extract of C. unshiu exhibited PL inhibitory properties through *in vitro* and *in vivo* studies [19].

In this research, compounds derived from the extracts of *C. aurantifolia*, *C. grandis*, *C. hystrix*, *C. medica* and *C. microcarpa*, sourced from their fruits, leaves, and peels were subjected to virtual screening through molecular docking simulations against PL. Compounds exhibiting strong potential against PL were subjected to a detailed analysis, considering their free energy of binding (FEB) and interactions within the active site of the PL. A thorough investigation was conducted on a total of 15 extracts from various plant components, including fruits, leaves, and peels, through *in vitro* bioassays to evaluate their inhibitory effects on PL. Hence, this study sought to determine the potential of selected citrus plants by combining computational approach with traditional plant extraction-based *in vitro* assays.

MATERIALS AND METHODS

Ligand and Protein Preparation

A total of 114 chemical compounds from five selected citrus namely *C. aurantifolia*, *C. grandis*, *C. hystrix*, *C. medica* and *C. microcarpa* were retrieved from several literature and journals (Table I). Throughout the search, Google Scholar, ScienceDirect and PubMed search engines were used with the following keywords "Phytochemical compound", "Polyphenols"; "Natural products" "Isolation"; "Identification"; "Characterisation"; "*Citrus aurantifolia*"; "Citrus grandis"; "Citrus hystrix"; "Citrus medica" and "Citrus microcarpa". The search for chemical compounds within the selected citrus fruits exclusively encompassed full research articles published in English.

Table I : List of chemical compounds from five selected citrus namely *C. aurantifolia*, *C. grandis*, *C. hystrix*, *C. medica* and *C. microcarpa*

Compound Code	Compound Name	Plant Part	Plant Sources	References
1	(E)-Caryophyllene	Leaves	*C. medica*	[36]
		Peels	*C. medica*	
2	(E)-Nerolidol	Leaves	*C. medica*	[36]
3	(E)-β-Farnesene	Leaves	*C. aurantifolia*	[36, 37]
			C. hystrix	
			C. medica	
		Peels	*C. aurantifolia*	
			C. grandis	
			C. hystrix	
			C medica	
			C. microcarpa	
4	(E)-β-Ocimene	Leaves	*C. medica*	[36]
		Peels	*C. medica*	
5	(Z)-Nerolidol	Leaves	*C. aurantifolia*	[37]
			C. grandis	
			C. hystrix	
			C. microcarpa	
		Peels	*C. aurantifolia*	
			C. hystrix	

Compound Code	Compound Name	Plant Part	Plant Sources	References
6	(Z)-β-Farnesene	Leaves	*C. aurantifolia* *C. grandis*	[37]
		Peels	*C. aurantifolia* *C. grandis* *C. hystrix* *C. microcarpa*	
7	(Z)-β-Ocimene	Leaves	*C. medica*	[36]
		Peels	*C. medica*	
8	1,8-Cineole	Leaves	*C. medica*	[36]
9	3,3′,4′,5,6,7,8-Heptamethoxyflavone	Leaves	*C. grandis*	[38]
10	6-Methylhept-5-en-2-one	Peels	*C. medica*	[36]
		Leaves	*C. medica*	
11	Acetylnaringin	Fruits	*C. grandis*	[33]
		Peels	*C. grandis*	
12	allo-Ocimene	Peels	*C. medica*	[36]
13	Apigenin	Leaves	*C. aurantifolia* *C. hystrix*	[39, 40]
		Peels	*C. aurantifolia*	
14	Apigenin-6-C-glucosyl-7-O-glucoside	Peels	*C. grandis*	[33]
15	Aromadendrene	Peels	*C. grandis* *C. microcarpa*	[37]
16	Caryophyllene oxide	Leaves	*C. medica*	[36]
17	Casticine	Peels	*C. medica*	[36]
18	cis-Limonene-1,2-epoxide	Leaves	*C. medica*	[36]
		Peels	*C. medica*	
19	cis-Linalool oxide	Peels	*C. hystrix*	[37]
20	cis-β-Ocimene	Leaves	*C. aurantifolia* *C. grandis*	[37]
21	Citronellal	Leaves	*C. hystrix* *C. medica*	[36, 37]
		Peels	*C. hystrix* *C. medica*	
22	Citronellol	Leaves	*C. hystrix* *C. medica*	[36, 37]
23	Citronellyl acetate	Leaves	*C. grandis* *C. hystrix* *C. medica*	[36, 37]
		Peels	*C. medica*	
24	Decanal	Leaves	*C. medica*	[36]
25	Didymin	Fruits	*C. grandis*	[33]
26	Diosmetin-6-C-glucoside	Fruits	*C. medica*	[32, 33]
		Peels	*C. grandis*	
27	Diosmetin-6,8-di-C-glucoside	Fruits	*C. medica*	[32]
		Peels	*C. medica*	
28	Diosmin	Fruits	*C. grandis* *C. medica*	[32, 36]
		Peels	*C. grandis* *C. hystrix* *C. medica*	

Compound Code	Compound Name	Plant Part	Plant Sources	References
29	Dodecanal	Leaves	*C. medica*	[36]
30	Elemol	Leaves	*C. aurantifolia* *C. hystrix* *C. microcarpa*	[37]
		Peels	*C. aurantifolia* *C. microcarpa*	
31	Eriodictyol-7-O-rutinoside	Fruits	*C. medica*	[32]
		Peels	*C. medica*	
32	Flavanomarein	Peels	*C. medica*	[36]
33	Geranial	Leaves	*C. aurantifolia* *C. grandis* *C. medica*	[36, 37]
		Peels	*C. aurantifolia* *C. grandis* *C. medica*	
34	Geranic acid	Leaves	*C. medica*	[36]
35	Geraniol	Leaves	*C. aurantifolia* *C. grandis* *C. medica*	[36, 37]
		Peels	*C. aurantifolia* *C. grandis* *C. medica*	
36	Geranyl acetate	Peels	*C. aurantifolia* *C. medica* *C. microcarpa*	[36, 37]
		Leaves	*C. aurantifolia* *C. hystrix* *C. medica* *C. microcarpa*	
37	Germacrene-D	Peels	*C. medica*	[36]
38	Hedycaryol	Leaves	*C. grandis* *C. hystrix* *C. microcarpa*	[37]
		Peels	*C. hystrix*	
39	Hesperetin	Fruits	*C. aurantifolia*	[39]
		Leaves	*C. hystrix*	
40	Hesperetin-7-O-neohesperidoside	Fruits	*C. aurantifolia* *C. medica* *C. microcarpa*	[32]
		Peels	*C. grandis* *C. hystrix* *C. medica* *C. microcarpa*	
41	Hesperidin	Fruits	*C. aurantifolia* *C. medica* *C. microcarpa*	[32, 40, 41]
		Leaves	*C. aurantifolia*	
		Peels	*C. aurantifolia* *C. hystrix* *C. medica* *C. microcarpa*	

Compound Code	Compound Name	Plant Part	Plant Sources	References
42	Hyperosid	Peels	*C. medica*	[36]
43	Isolimonexic acid	Fruits	*C. aurantifolia*	[42]
44	Isorhamnetin	Leaves	*C. hystrix*	[39]
45	Kaempferol	Leaves	*C. aurantifolia*	[40]
		Peels	*C. aurantifolia*	
46	Limonene		*C. aurantifolia*	[36, 37, 43]
			C. grandis	
			C. hystrix	
			C. medica	
		Peels	*C. microcarpa*	
			C. aurantifolia	
			C. grandis	
			C. hystrix	
			C. medica	
			C. microcarpa	
47	Limonexic acid	Fruits	*C. aurantifolia*	[42]
48	Limonin	Fruits	*C. aurantifolia*	[42]
49	Linalool	Leaves	*C. aurantifolia*	[36, 37]
			C. hystrix	
			C. medica	
			C. microcarpa	
		Peels	*C. grandis*	
			C. hystrix	
			C. medica	
			C. microcarpa	
50	Lucenin-2	Peels	*C. grandis*	[33]
51	Luteolin	Leaves	*C. hystrix*	[36, 39]
		Peels	*C. medica*	
52	Melitidin	Fruits	*C. grandis*	[33]
		Peels		
53	Myrcene	Leaves	*C. medica*	[36, 37]
			C. microcarpa	
		Peels	*C. medica*	
			C. microcarpa	
54	Myricetin	Leaves	*C. hystrix*	[39]
55	Naringin	Fruits	*C. grandis*	[33, 41, 44]
		Leaves	*C. grandis*	
		Peels	*C. grandis*	
56	Narirutin	Peels	*C. medica*	[36]
57	Natsudaidain	Leaves	*C. grandis*	[44]
58	Neodiosmin	Leaves	*C. grandis*	[44]
59	Neoeriocitrin	Fruits	*C. grandis*	[33, 44]
		Leaves	*C. grandis*	
		Peels	*C. grandis*	
60	Neral	Leaves	*C. aurantifolia*	[36, 37]
			C. grandis	
			C. medica	
		Peels	*C. aurantifolia*	
			C. grandis	
			C. medica	

Compound Code	Compound Name	Plant Part	Plant Sources	References
61	Nerol	Leaves	*C. aurantifolia* *C. grandis* *C. medica*	[36, 37]
		Peels	*C. medica*	
62	Neryl acetate	Peels Leaves	*C. medica*	[36]
63	Nobiletin	Fruits	*C. hystrix* *C. aurantifolia* *C. grandis* *C. microcarpa*	[36, 40, 41, 44]
		Peels	*C. aurantifolia* *C. hystrix* *C. medica*	
64	Nonanal	Leaves	*C. medica*	[36]
65	Octanal	Leaves	*C. medica*	[36]
66	Octanol	Leaves	*C. medica*	[36]
67	p-Cymene	Leaves Peels	*C. medica* *C. medica*	[36]
68	Peonidin	Leaves	*C. hystrix*	[39]
69	Phloretin-3′,5′-di-C-glucoside	Fruits	*C. medica* *C. microcarpa*	[32]
		Peels	*C. medica* *C. microcarpa*	
70	Phytol	Leaves	*C. aurantifolia* *C. grandis* *C. microcarpa*	[37]
		Peels	*C. grandis* *C. hystrix*	
71	Piperitone	Leaves	*C. medica*	[36]
72	Quercetin	Leaves	*C. aurantifolia* *C. hystrix*	[39, 40]
		Peels	*C. aurantifolia*	
73	Retusin	Peels	*C. medica*	[36]
74	Rhoifolin	Fruits Leaves Peels	*C. grandis* *C. grandis* *C. grandis*	[33, 44]
75	Robinetin trimethylether	Peels	*C. medica*	[36]
76	Rutin	Fruits Leaves Peels	*C. aurantifolia* *C. aurantifolia* *C. aurantifolia* *C. medica*	[36, 40]
77	Sabinene	Leaves	*C. aurantifolia* *C. grandis*	[36, 37]
		Peels	*C. medica* *C. medica*	
78	Sinensetin	Fruits Peels	*C. hystrix* *C. hystrix* *C. medica*	[36, 41]

Compound Code	Compound Name	Plant Part	Plant Sources	References
79	Tangeretin	Fruits Leaves Peels	*C. hystrix* *C. aurantifolia* *C. hystrix* *C. medica*	[36, 40, 41]
80	Terpinen-4-ol	Leaves Peels	*C. medica* *C. microcarpa* *C. aurantifolia* *C. grandis* *C. hystrix* *C. medica* *C. microcarpa*	[36, 37]
81	Terpinolene	Leaves Peels	*C. grandis* *C. medica* *C. hystrix* *C. medica* *C. microcarpa*	[36, 37]
82	trans-Limonene-1,2-epoxide	Leaves	*C. medica*	[36]
83	trans-Nerolidol	Peels	*C. medica*	[36]
84	trans-Sabinene hydrate	Leaves Peels	*C. hystrix* *C. medica*	[36, 37]
85	trans-α-Bergamotene	Peels	*C. aurantifolia* *C. medica*	[36, 37]
86	trans-β-Ocimene	Leaves	*C. aurantifolia* *C. grandis* *C. hystrix* *C. microcarpa*	[37]
87	Undecanal	Leaves	*C. medica*	[36]
88	Vicenin-2	Fruits Peels	*C. grandis* *C. microcarpa* *C. grandis*	[32, 33]
89	α-Bisabolene	Peels	*C. medica*	[36]
90	α-Bisabolol	Leaves Peels	*C. medica* *C. medica*	[36]
91	α-Cadinene	Leaves Peels	*C. grandis* *C. hystrix* *C. hystrix*	[37]
92	α-Eudesmol	Leaves Peels	*C. aurantifolia* *C. grandis* *C. hystrix* *C. microcarpa* *C. aurantifolia* *C. grandis* *C. hystrix*	[37]
93	α-Guaiene	Leaves Peels	*C. aurantifolia* *C. grandis* *C. microcarpa*	[37]

Compound Code	Compound Name	Plant Part	Plant Sources	References
94	α-Humulene	Leaves	*C. aurantifolia* *C. grandis* *C. hystrix* *C. microcarpa*	[37]
		Peels	*C. aurantifolia* *C. hystrix*	
95	α-Phellandrene	Leaves Peels	*C. microcarpa* *C. grandis* *C. medica* *C. microcarpa*	[36, 37]
96	α-Pinene	Leaves	*C. medica* *C. microcarpa*	[36, 37]
		Peels	*C. aurantifolia* *C. grandis* *C. hystrix* *C. medica* *C. microcarpa*	
97	α-Selinene	Leaves	*C. microcarpa*	[37]
98	α-Sesqui-phellandrene	Leaves	*C. microcarpa*	[37]
99	α-Sinensal	Peels	*C. hystrix*	[37]
100	α-Terpinene	Peels	*C. medica*	[36]
101	α-Terpineol	Leaves	*C. medica* *C. microcarpa*	[36, 37]
		Peels	*C. aurantifolia* *C. grandis* *C. medica* *C. microcarpa*	
102	α-Thujene	Leaves	*C. medica*	[37]
		Peels	*C. medica*	
103	β-Bisabolene	Leaves	*C. aurantifolia* *C. medica*	[36, 37]
		Peels	*C. medica*	
104	β-Caryophyllene	Leaves	*C. aurantifolia* *C. grandis* *C. hystrix* *C. microcarpa*	[37]
		Peels	*C. aurantifolia* *C. grandis* *C. hystrix* *C. microcarpa*	
105	β-Cubebene	Leaves	*C. hystrix*	[37]
106	β-Elemene	Leaves	*C. microcarpa*	[37]
107	β-Eudesmol	Leaves	*C. aurantifolia* *C. grandis* *C. hystrix* *C. microcarpa*	[37]
		Peels	*C. aurantifolia* *C. hystrix* *C. microcarpa*	

Compound Code	Compound Name	Plant Part	Plant Sources	References
108	β-Myrcene	Leaves	*C. aurantifolia* *C. hystrix*	[37]
		Peels	*C. aurantifolia* *C. grandis* *C. hystrix*	
109	β-Pinene	Leaves	*C. aurantifolia* *C. grandis* *C. hystrix* *C. medica* *C. microcarpa*	[37, 43]
		Peels	*C. aurantifolia* *C. grandis* *C. hystrix* *C. medica* *C. microcarpa*	
110	γ-Cadinene	Leaves	*C. grandis*	[37]
111	γ-Terpinene	Leaves	*C. hystrix* *C. medica*	[37, 43]
		Peels	*C. aurantifolia* *C. grandis* *C. hystrix* *C. medica* *C. microcarpa*	
112	δ-3-Carene	Leaves	*C. grandis* *C. hystrix* *C. medica*	[36, 37]
		Peels	*C. aurantifolia* *C. hystrix*	
113	δ-Cadinene	Leaves	*C. hystrix* *C. microcarpa*	[37]
		Peels	*C. hystrix*	
114	δ-Elemene	Peels	*C. microcarpa*	[37]
		Leaves	*C. microcarpa*	

The two-dimensional structures of the retrieved compounds were sketched using ACD/ChemSketch software and then converted into pdbqt format using Raccoon.py script [25]. The crystal structure of PL was obtained from the Protein Data Bank (PDB ID: 1LPB, resolution; 2.46 Å) [26]. The water molecules and their co-crystallized compounds were removed from the protein structure and polar hydrogen atoms as well as Kollman charges were added to the structure using AutoDock Tools (ADT) version 1.5.6 [27], a graphical user interface for AutoDock 4.2 and also part of MGLTools [28]. The protonation states of the protein's ionizable groups were determined using the PROPKA3 empirical pKa predictor [29].

Control docking and virtual screening

Methoxyundecylphosphinic acid (MUP) which was obtained from the complex 1LPB was docked inside the active PL site using AutoDock Vina (Trott & Olson, 2010). The docking was carried out at the center of the catalytic binding site of the lipase with the coordinates of 8.692, 22.943, 52.624 as x, y, z in Cartesian coordinates with a grid box of 25 x 25 x 25 Å and a grid spacing of 1.0 Å. The potential chemical compounds from the selected citrus plants and orlistat as the control were docked into the PL by using AutoDock Vina with the same parameters as the control docking simulation.

Plant collection and extraction

Fruits and leaves from five specific citrus varieties were collected across different regions of Peninsular Malaysia. Among them, *C. hystrix* and *C. microcarpa* were sourced from Kampung Raja, Besut, Terengganu. Meanwhile, we obtained C. maxima fruits from Ipoh, Perak, *C. medica* from Kampung Kuar Luar, Pengkalan Hulu, Perak, and *C. aurantifolia* from Baling, Kedah. The leaves of these selected citrus species,

were ground into a fine powder and subjected to maceration using 80% methanol over a period of three days. The resulting solution was then concentrated using a rotary evaporator. In the case of the fruits, their juices were extracted and ethyl acetate added to facilitate the extraction process. The extracted fruit compounds were combined, concentrated, and subsequently stored at -20°C in a freezer for future use.

***In vitro* pancreatic lipase inhibition bioassay**

The pancreatic lipase inhibition activity was assessed using the Lipase Activity Assay Kit II (MAK047) according to the manufacturer's instructions (SIGMA). A total of 100µL of the Master Reaction Mix was added to each sample as well as positive control into a 96-well plate, ensuring thorough mixing with a shaker. The initial absorbance reading was measured at 412 nm using the GloMax®-Multi Detection System microplate reader after which the plate was incubated in the Thermo Shaker Incubator MB1004A at 37 °C for 15 minutes. Following the incubation period, Lipase Substrate was added into each well and the mixture was again measured at the same wavelength. The negative control was also included to determine the inhibitory activity.

RESULTS

In-silico molecular docking

(a) Quantitative analysis – binding energy

Table II summarizes the Free Energy of Binding (FEB) and binding interaction of MUP, orlistat and predicted high inhibitory activity compounds. Redocking of MUP against PL demonstrated that the most favorable conformation achieved a binding energy of -6.70 kcal/mol with a reference RMSD value of 1.97 Å. An RMSD value below 2.00 Å indicates minimal deviation from the original pose, signifying that the docking parameters effectively replicate the original docking process [30, 31].

Table II : The free energy binding (FEB) and interaction types of MUP, Orlistat and predicted high inhibitory activity compounds

Code	Name	Free Energy Binding (kcal/mol)	Interaction Types	Key Amino Acids			Other Amino Acids
				Ser152	His263	Asp176	
26	Diosmetin 6-C-glucoside	-12.2	Hydrogen	1	1	-	3
			Hydrophobic	-	-	-	9
55	Naringenin 7-O-neohesperidoside	-10.6	Hydrogen	1	-	-	2
			Hydrophobic	-	-	-	10
40	Hesperetin-7-O-neohesperidoside	-10.4	Hydrogen	1	-	-	2
			Hydrophobic	-	-	-	11
74	Rhoifolin	-10.4	Hydrogen	1	-	-	3
			Hydrophobic	-	-	-	9
59	Neoeriocitrin	-10.3	Hydrogen	1	-	-	4
			Hydrophobic	-	-	-	9
58	Neodiosmin	-10.2	Hydrogen	1	-	-	6
			Hydrophobic	-	-	-	9
14	Apigenin 6-C-glucosyl-7-O-glucoside	-10.0	Hydrogen	1	1	-	3
			Hydrophobic	-	-	-	10
88	Vicenin-2	-10.0	Hydrogen	1	1	-	2
			Hydrophobic	-	-	-	11
MUP	Methoxyundecyl phosphinic acid	-6.70	Hydrogen	-	-	-	2
			Hydrophobic	-	1	-	4
			Covalent	1	-	-	-
Orlistat (control)	Orlistat	-7.20	Hydrogen	-	1	-	2
			Hydrophobic	-	-	-	14
			Covalent	1	-	-	-

Orlistat which is one of the drugs approved by the US FDA was also docked against the PL to understand its interactions and FEB. The docking simulation of orlistat against PL had given a FEB of -7.20 kcal/mol which is lower than the co-crystallized ligand.

The selected citrus compounds were effectively docked within the PL pocket, exhibiting a range of FEB from -12.20 kcal/mol to -4.60 kcal/mol. These compounds were categorized into three distinct groups based on their FEB values. The first group encompassed compounds with a high predicted inhibitory potential against PL, falling within the range of -12.20 kcal/mol to -10.00 kcal/mol. The second group included compounds displaying moderate inhibitory activity, with FEB values ranging from -9.00 to -7.00 kcal/mol. Lastly, the third group comprised compounds predicted to have low inhibitory activity, with FEB values spanning from -6.00 to -4.00 kcal/mol. Notably, in this study we only discuss the compounds which predicted to possess high inhibitory activity against PL exhibited stronger binding affinities when compared to MUP and orlistat. These findings suggest that eight citrus compounds hold promising potential as PL inhibitors, given their superior affinities relative to the control substances. They are compounds 14 (Apigenin 6-C-glucosyl-7-O-glucoside), 26 (Diosmetin 6-C-glucoside), 40 (Hesperetin-7-O-neohesperidoside), 55 (Naringin), 58 (Neodiosmin), 59 (Neoeriocitrin), 74 (Neoeriocitrin), and 88 (Vicenin-2).

(b) Qualitative analysis – binding interaction

Figure 1 illustrates the positioning of both crystallized and redocked MUP compounds within the active site of PL, indicating their potential interactions with the same amino acid residues. A detailed view of their 2D interactions, generated using the LigPlot program, is presented in Figure 2. In the case of crystallized MUP, it formed two hydrogen bonds, one with Gly76 at a distance of 3.11 Å and another with Phe77 at 2.85 Å. Additionally, hydrophobic interactions occurred with Gly76, His151, Ala178, Pro180, Phe215, and His263. Conversely, as depicted in Figure 2, redocked MUP interacted with PL via hydrogen bonds with Phe77 at a distance of 3.12 Å and Leu153 at a distance of 2.87 Å, respectively. It also established a network of hydrophobic interactions involving amino acids Tyr114, Ala178, Phe215, His263, and Gly276. Remarkably, both crystallized and redocked MUP compounds formed a hydrogen bond with Phe77 and shared hydrophobic interactions with Ala178, Phe215, His263, in addition to a covalent bond with the amino acid Ser152. These consistent interactions with similar amino acid residues in both compounds elucidate their placement within the same binding site, as depicted in Figure 1.

The 2D interactions of the predicted high inhibitory activity compounds and orlistat are illustrated in

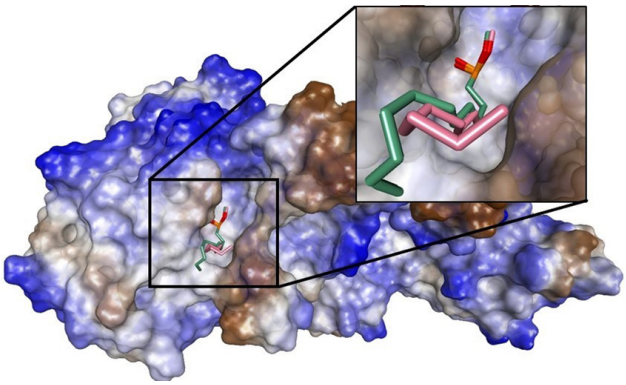

Figure 1 : The 3D orientation of crystal and redocked methoxyundecylphosphinic acid (MUP) inside the active site of pancreatic lipase (PL). The pink compound represents the crystal MUP while the green compound represents the redocked MUP.

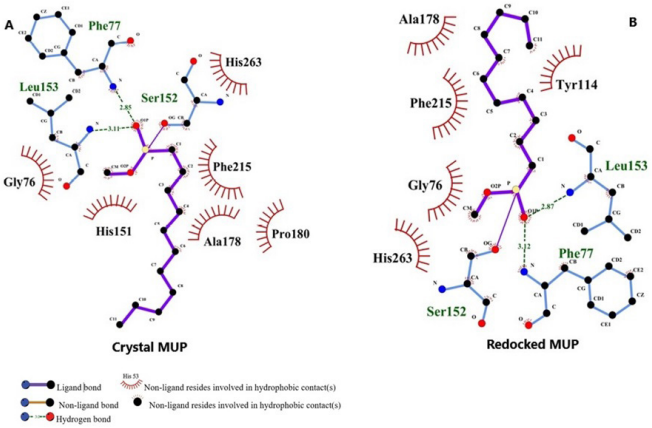

Figure 2 : The 2D interaction of (A) crystal MUP and (B) redocked MUP within the pancreatic lipase active site. The green dotted line represents the hydrogen bond interaction, the straight purple line represents the covalent bond and the red half-circle represents the hydrophobic interaction.

Figures 3 and 4. Figure 3A depicts the 2D interaction of orlistat with PL. Notably, the ketone group of beta lactone from orlistat was observed to form a covalent bond with the amino acid Ser152, consistent with previous research findings that the mode of action of orlistat is attributable to this covalent interaction with Serine [20, 32]. Further inspection of the binding interactions revealed that orlistat established three hydrogen bonds, each with Gly76 (at 3.00 Å), His151 (at 2.87 Å), and His263 (at 3.02 Å). Additionally, this control ligand engaged in hydrophobic interactions with a total of twelve amino acid residues, specifically Phe77, Ile78, Asp79, Tyr114, Leu153, Ala178, Pro180, Thr255, Arg256, Ala259, Ala260, and Leu264.

Figure 3B provides insight into the 2D interaction between compound 26 and PL. Compound 26 exhibited noteworthy binding interactions, establishing five hydrogen bonds with Phe77 (at 3.21 Å), Ser152 (at 3.13

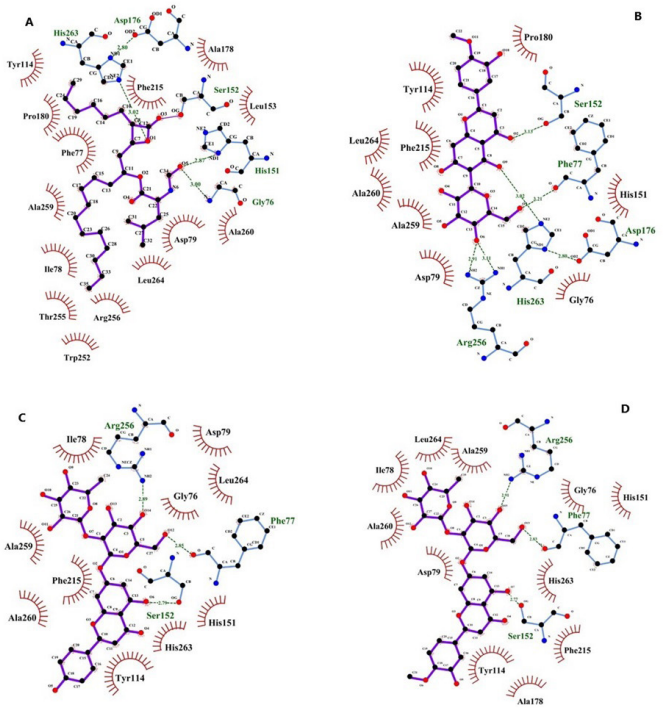

Figure 3 : The 2D interaction of (A) orlistat, (B) compound 26, (C) compound 55 and (D) compound 40, within the active site of the pancreatic lipase. The purple straight line represents the covalent bond, the green dash line represents the hydrogen bond while red half-circle represents the hydrophobic interaction.

Å), Arg256 (at 2.91 Å and 3.11 Å), and His263 (at 3.02 Å). Furthermore, this compound actively participated in hydrophobic interactions with a total of nine amino acid residues, specifically involving Gly76, Asp79, Tyr114, His 151, Pro180, Phe215, Ala259, Ala260, and Leu264.

Figure 3C illustrates the 2D interaction of compound 55 with PL. Compound 55 exhibited binding interactions involving three hydrogen bonds, establishing connections with Phe77 (at 2.85 Å), Ser152 (at 2.79 Å), and Arg256 (at 2.89 Å). Furthermore, this ligand participated in hydrophobic interactions with a total of ten amino acid residues, namely Gly76, Ile78, Asp79, Tyr114, His151, Phe215, Ala259, Ala260, His263, and Leu264.

Figure 3D depicts the 2D interaction of compound 40 with PL. Compound 40 exhibited binding interactions characterized by three hydrogen bonds, formed with Phe77 (at 2.83 Å), Ser152 (at 2.77 Å), and Arg256 (at 2.91 Å). Furthermore, this ligand engaged in hydrophobic interactions with a total of eleven amino acid residues, specifically Gly76, Ile78, Asp79, Tyr114, His151, Ala178, Phe215, Ala259, Ala260, His263, and Leu264.

Figure 4A illustrates the 2D interaction between compound 74 and PL. Compound 74 exhibited robust

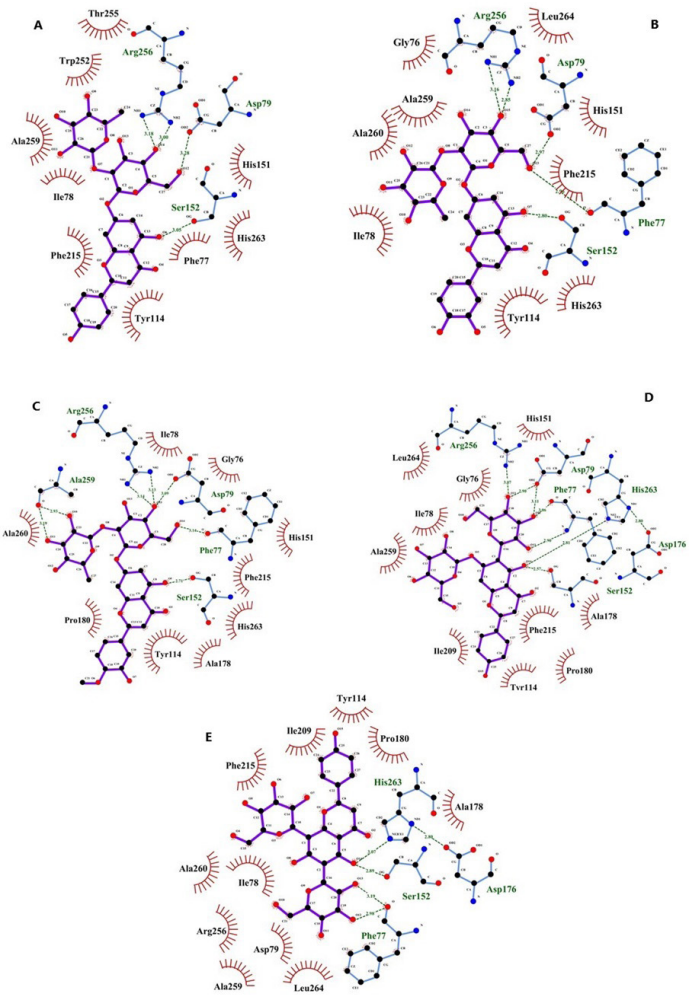

Figure 4 : The 2D interaction of (A) compound 74, (B) compound 59, (C) compound 58, (D) compound 14 and (E) compound 88. The green dash line represents the hydrogen bond while the red half-circle represents the hydrophobic interactions.

binding interactions, forming four hydrogen bonds, including ones with Asp79 (at 3.28 Å), Ser152 (at 3.05 Å), and Arg256 (at 3.18 Å and 3.09 Å). Additionally, this compound engaged in hydrophobic interactions with a total of nine amino acid residues, specifically Phe77, Ile78, Tyr114, His151, Phe215, Trp252, Thr255, Ala259, and His263.

Figure 4B depicts the 2D interaction of compound 59 with PL. Compound 59 demonstrated binding interactions with five hydrogen bonds, each with Phe77 (at 2.98 Å), Asp79 (at 2.97 Å), Ser152 (at 2.80 Å), and Arg256 (at 3.16 Å and 2.85 Å). Additionally, this ligand engaged in hydrophobic interactions with a total of nine amino acid residues, specifically Gly76, Ile78, Tyr114, His151, Phe215, Ala259, Ala260, His263, and Leu264.

In Figure 4C, the 2D interaction between compound 58 and PL is depicted. Compound 58 displayed a series of binding interactions, forming seven hydrogen bonds with Phe77 (at 3.14 Å), Asp79 (at 3.09 Å), Ser152 (at

2.71 Å), Arg256 (at 3.18 Å and 3.13 Å), and Ala259 (at 3.19 Å and 2.93 Å). Moreover, this ligand actively engaged in hydrophobic interactions with a total of nine amino acid residues, specifically Gly76, Ile78, Tyr114, His151, Ala178, Pro180, Phe215, Ala260, and His263.

Figure 4D presents the 2D interaction profile between compound 14 and PL. Compound 14 displayed substantial binding interactions, establishing seven hydrogen bonds, including those with Phe77 (at 2.90 Å and 3.06 Å), Asp79 (at 2.90 Å and 3.11 Å), Ser152 (at 2.57 Å), Arg256 (at 3.07 Å), and His263 (at 2.81 Å). Furthermore, this ligand actively participated in hydrophobic interactions involving a total of nine amino acid residues, specifically Gly76, Ile78, Tyr114, His151, Phe215, Ala259, Ala260, His263, and Leu264.

Figure 4E illustrates the 2D interaction between compound 88 and PL. Compound 88 exhibited binding interactions characterized by four hydrogen bonds, forming connections with Phe77 (at 2.98 Å and 3.19 Å), Ser152 (at 2.89 Å), and His263 (at 3.07 E). Additionally, this compound actively participated in hydrophobic interactions with a total of eleven amino acid residues,

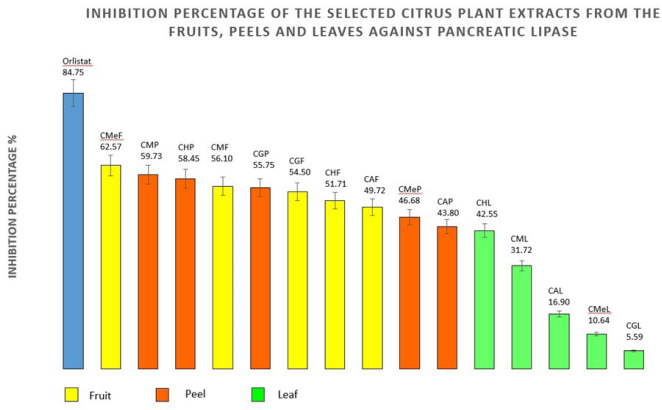

Figure 5 : Comparison of inhibition percentage of peels, leaves and fruits parts of Citrus plants (CM: *C. microcarpa*, CH: *C. hystrix*, CG: *C. grandis*, CMe: *C. medica*, CA: *C. aurantifolia*) extracts against the pancreatic lipase.

specifically Ile78, Asp79, Tyr114, Ala178, Pro180, Ile209, Phe215, Arg256, Ala259, Ala260, and Leu264.

***In vitro* bioassay of citrus plant extracts on pancreatic lipase inhibition**

As shown in Figure 5, the citrus plant extracts from peels, leaves and fruits show moderate to low inhibitory activity on the PL compared to the control, orlistat, with an inhibition percentage of 84.75%. The highest inhibition was from the fruit extract of *C. medica* with an inhibition percentage of 62.57 %, followed by the peel extracts of *C. microcarpa* with an inhibition percentage of 59.73%, and *C. hystrix* with an inhibition percentage of 58.45%, subsequently followed by fruit extract of *C. microcarpa* with an inhibition percentage of 56.10%, the peel and fruit extracts of *C. grandis* with inhibition percentages of 55.75% and 54.50% respectively, the fruit extract of *C. hystrix* with an inhibition percentage of 51.71%, the fruit extract of *C. aurantifolia* with an inhibition percentage of 49.72%, the peel extract of *C. medica* with an inhibition percentage of 46.68%, the peel extract of *C. aurantifolia* with an inhibition percentage of 43.80% and lastly the leaf extracts of *C. hystrix*, *C. microcarpa*, *C. aurantifolia*, *C. medica* and *C. grandis* with inhibition percentages of 42.55%, 31.72%, 16.90%, 10.64% and 5.59%, respectively.

DISCUSSION

The validation of docking parameters has been performed by redocking of PL with its co-crystallized ligand, MUP. The results of redocking MUP within the active site of the PL revealed a minor deviation of 1.97 Å from the original crystal MUP orientation. This deviation, less than 2.00 Å, indicates a close alignment between the molecular docking parameters employed for redocking MUP and those utilized for docking the crystal MUP, as previously documented [30]. Furthermore, we compared the interactions of redocked MUP with the catalytic triads of the PL, involving residues Ser152, Asp176, and His263 with the crystal structure of MUP. Notably, Ser152 emerged as the key amino acid in the lipolytic activity of the PL.

The diagrams of the 2D interactions between the small compounds and the PL have been generated using LigPlot program. LigPlot illustrates the patterns of hydrogen-bond interactions and hydrophobic contacts occurring between the ligand(s) and various elements of the protein, including both its main-chain and side-chain components. This system is capable to graphically represent related sets of interactions between ligands and proteins in a consistent orientation. This functionality greatly aids in various research tasks, such as the analysis of multiple small molecules binding to a common protein target, the interaction of a single ligand with homologous proteins, or the broader scenario in which both the protein and the ligand undergo changes.

Based on the results, the redocked MUP exhibited a covalent bond with the Ser152 residue, mirroring the interaction seen in the crystal MUP binding to PL. This interaction aligns with the findings of Egloff and colleagues, who observed that the phosphorous atom of the crystal MUP forms a covalent bond with the Ser152 residue of PL [26]. Additionally, both the crystal and redocked MUP formed a hydrogen bond with the Phe77 residue of PL. It's worth noting that Phe77 plays a crucial role as one of the oxyanion holes, stabilizing the protein-ligand complex, as described by Egloff et al. (1995) [26]. Given the comparable RMSD value and interactions observed between the redocked MUP and PL when compared to the crystal MUP, we can

confidently affirm the validation of the redocked MUP's docking parameters. These validated parameters were subsequently employed in the virtual screening of isolated compounds from the selected citrus plants.

In this study, we selected orlistat, an FDA-approved drug utilized to inhibit PL, as our control. A molecular docking simulation of orlistat with PL was conducted to gain insights into its binding orientation and affinity. The results of the docking revealed that orlistat exhibited an FEB of -6.90 kcal/mol, surpassing the FEB of MUP, which scored at -6.70 kcal/mol. This heightened binding affinity of orlistat in comparison to MUP has been corroborated by a study indicating that orlistat is three times more potent than MUP as a PL inhibitor [33]. Furthermore, we observed that the ketone group within the beta lactone ring of orlistat established a covalent bond with the Ser152 residue of PL.

The covalent bond formation between orlistat and the Ser152 residue of PL resembles the interaction observed between MUP and PL. This type of interaction with the Ser152 residue plays a crucial role in inhibiting the lipolytic activities of PL, as indicated by Veeramachaneni and fellow researchers [34]. To further enhance the orlistat-pancreatic lipase complex stability, the methoxy group within the beta lactone ring of orlistat established a hydrogen bond with the His263 residue of PL, which is one of the catalytic triad residues responsible for the lipolytic activities of PL. The potential PL inhibitors, derived from extracts of peels, leaves, and fruits of *C. microcarpa*, *C. hystrix*, *C. medica*, *C. grandis* and *C. aurantifolia* were identified by using an in-silico molecular docking approach. This method involved predicting the orientation and binding affinity of the compounds against PL.

As outlined in Table 2, a total of eight compounds exhibited significant inhibitory potential against PL, displaying superior affinity compared to the control, with FEB values ranging from -12.20 kcal/mol to -10.00 kcal/mol. In the case of all these compounds, they established a single hydrogen bond with the Ser152 residue within PL. However, compounds 26, 14, and 88 were noteworthy as they formed a hydrogen bond not only with Ser152 but also with His263, both of which are vital components within the catalytic triads of PL. Remarkably, all eight compounds predicted to exhibit strong inhibition against PL shared a common structural scaffold derived from the flavonoid class.

This particular scaffold has demonstrated effective inhibitory activity against PL. For example, hesperidin, a citrus flavonoid isolated from C. unshiu peels, exhibited notable PL inhibitory activity with an IC50 of 32 µg/ml. Notably, it was observed that the hydroxy groups on the phenol ring within the flavonoid structure of all eight compounds derived from those selected citrus plants were actively engaged in forming hydrogen bonds with the Ser152 residue in PL. Furthermore, these eight compounds, including orlistat, established at least one hydrogen bond with key amino acids, with the exception of MUP. The catalytic triad of PL comprises Ser152, Asp176, and His263, with Ser152 being the most pivotal residue in facilitating the lipolytic activity of pancreatic lipase [34].

Consequently, compounds capable of interacting with Ser152 may indicate their capability to inhibit the lipolytic activity of PL. Compound 26, also known as diosmetin 6-C-glucoside, emerged as the top-ranking compound among the eight predicted to possess high PL inhibitory activity, exhibiting an FEB of -12.2 kcal/mol. This compound can be isolated from both the fruit extract of *C. medica* and the peel extract of *C. grandis*. Compound 26 established one hydrogen bond each with both Ser152 and His263 residues within PL. Results from *in vitro* studies revealed that the fruit extract of *C. medica* exhibited the highest PL inhibitory activity, displaying an impressive inhibition percentage of 62.59%.

It has been noted that compound 26 is found within the fruit extract of *C. medica*. Consequently, it is hypothesized that the enhanced inhibition observed in the *C. medica* fruit extract could likely be attributed to the presence of compound 26, which was predicted to exhibit the highest inhibitory activity against PL. Compound 26 is a C-glycosidic flavone, obtainable from both the fruit of *C. medica* and the peel extracts of *C. grandis*, as documented in studies by Roowi & Crozier (2011) and Zhang et al. (2014) [35, 36]. Previous research has highlighted the potent inhibitory activity of this flavone class on PL, as demonstrated by Lee and colleagues [37]. Additionally, the *C. grandis* leaf extract contains a total of four compounds - namely compounds 55, 74, 59, and 58 - predicted to possess significant inhibitory activities against PL.

Compound 58 secured the sixth position among the eight compounds categorized within the high inhibitory activity group. It distinguishably formed the greatest number of hydrogen bonds when compared to the other seven compounds in the same high activity group, establishing a total of seven hydrogen bonds within the PL's active site. A higher count of hydrogen bonds in the protein-ligand complex often signifies robust inhibition of the compound against the protein target [38]. Nevertheless, in contrast to its promising *in silico* inhibitory activity, the leaf extract of *C. grandis* displayed the lowest inhibition among the compounds when assessed *in vitro*, registering an inhibition percentage of 5.59%. It is worth noting that despite compound 58 establishing the most significant number of hydrogen bonds with PL, the *in vitro* assessment of the inhibitory activity in the *C. grandis* leaf extract exhibited the lowest inhibition percentage. This discrepancy may be attributed to the fact that interactions between compound 58 and

PL resulted in the formation of only one hydrogen bond with the critical amino acids. This outcome highlights the crucial significance of interactions formed between compounds and the key amino acids within the protein target.

CONCLUSION

Following the results, eight compounds were identified with significant inhibitory potential against PL through molecular docking, with diosmetin 6-C-glucoside ranking as the highest-scoring compound. Subsequent *in vitro* studies on chosen citrus extracts confirmed the outcomes of the molecular docking, highlighting *C. medica* fruit extract as exhibiting the most potent inhibition, with published data of the presence of diosmetin 6-C-glucoside predicted in this extract. The collective results from both *in silico* and *in vitro* methods, in conjunction with existing literature, strongly suggest that diosmetin 6-C-glucoside holds promise as a potential PL inhibitor. Further investigations, including isolation and *in vitro* bioassay assessments of these potential inhibitors, are warranted to validate their inhibitory capabilities against PL.

AUTHOR CONTRIBUTIONS

K.N.A.R.: writing, reviewing and editing the original draft; S.H.: lab work, methodology, software, data analysis, visualisation and writing original draft; S.Z.M.Z.: supervision, reviewing and editing the original draft; A.A.A.N.: methodology, data analysis; N.N.I.: methodology, data analysis; S.M.: supervision; S.R.: methodology, data analysis; H.A.W.: provided the computational laboratory facilities to perform this study; E.E.K.: supervision, conceptualisation, methodology, writing, reviewing and editing the manuscript and project administration.

ACKNOWLEDGEMENT

We are thankful to Universiti Sains Malaysia for the Research University Individual Grant [RUI Grant: Grant No. 1001/PFARMASI/811330] with the title of "Identification and Evaluation of Synthetic and Phytochemical Compounds for Lipase Inhibitor Activity", which provided support for this research.

REFERENCES

1. San-Cristobal, R., et al., Contribution of macronutrients to obesity: implications for precision nutrition. Nat Rev Endocrinol, 2020. 16(6): p. 305-320.
2. Torres-Carot, V., A. Suárez-González, and C. Lobato-Foulques, The energy balance hypothesis of obesity: do the laws of thermodynamics explain excessive adiposity? Eur J Clin Nutr, 2022. 76(10): p. 1374-1379.
3. Buchholz, T. and M.F. Melzig, Medicinal Plants Traditionally Used for Treatment of Obesity and Diabetes Mellitus - Screening for Pancreatic Lipase and α-Amylase Inhibition. Phytother Res, 2016. 30(2): p. 260-6.
4. Korhonen, P.E., et al., Both lean and fat body mass associate with blood pressure. Eur J Intern Med, 2021. 91: p. 40-44.
5. Erridge, S., et al., Obstructive Sleep Apnea in Obese Patients: a UK Population Analysis. Obes Surg, 2021. 31(5): p. 1986-1993.
6. Shapiro, J.A., et al., Fate of the Morbidly Obese Patient Who Is Denied Total Joint Arthroplasty. J Arthroplasty, 2020. 35(6s): p. S124-s128.
7. Jura, M. and L.P. Kozak, Obesity and related consequences to ageing. Age (Dordr), 2016. 38(1): p. 23.
8. Salvestrini, V., C. Sell, and A. Lorenzini, Obesity May Accelerate the Aging Process. Front Endocrinol (Lausanne), 2019. 10: p. 266.
9. Caballero, B., Humans against Obesity: Who Will Win? Adv Nutr, 2019. 10(suppl_1): p. S4-s9.
10. Cooper, A.J., et al., Sex/Gender Differences in Obesity Prevalence, Comorbidities, and Treatment. Curr Obes Rep, 2021. 10(4): p. 458-466.
11. Foster, C., et al., Physical activity and family-based obesity treatment: a review of expert recommendations on physical activity in youth. Clin Obes, 2018. 8(1): p. 68-79.
12. Bessesen, D.H. and L.F. Van Gaal, Progress and challenges in anti-obesity pharmacotherapy. Lancet Diabetes Endocrinol, 2018. 6(3): p. 237-248.
13. de la Garza, A.L., et al., Natural inhibitors of pancreatic lipase as new players in obesity treatment. Planta Med, 2011. 77(8): p. 773-85.
14. Montan, P.D., et al., Pharmacologic therapy of obesity: mechanisms of action and cardiometabolic effects. Ann Transl Med, 2019. 7(16): p. 393.
15. Avgerinos, K.I., et al., Obesity and cancer risk: Emerging biological mechanisms and perspectives. Metabolism, 2019. 92: p. 121-135.
16. Wen, X., et al., Signaling pathways in obesity: mechanisms and therapeutic interventions. Signal Transduct Target Ther, 2022. 7(1): p. 298.
17. Lustig, R.H., et al., Obesity I: Overview and molecular and biochemical mechanisms. Biochem Pharmacol, 2022. 199: p. 115012.
18. Birari, R.B. and K.K. Bhutani, Pancreatic lipase inhibitors from natural sources: unexplored potential. Drug Discov Today, 2007. 12(19-20): p. 879-89.
19. Kawaguchi, K., et al., Hesperidin as an inhibitor of lipases from porcine pancreas and Pseudomonas. Biosci Biotechnol Biochem, 1997. 61(1): p. 102-4.
20. Heck, A.M., J.A. Yanovski, and K.A. Calis, Orlistat, a new lipase inhibitor for the management of obesity. Pharmacotherapy, 2000. 20(3): p. 270-9.
21. Henness, S. and C.M. Perry, Orlistat: a review of

its use in the management of obesity. Drugs, 2006. 66(12): p. 1625-56.
22. Kumar, A. and S. Chauhan, Pancreatic lipase inhibitors: The road voyaged and successes. Life Sci, 2021. 271: p. 119115.
23. Velmurugan, D., R. Pachaiappan, and C. Ramakrishnan, Recent Trends in Drug Design and Discovery. Curr Top Med Chem, 2020. 20(19): p. 1761-1770.
24. Wang, X., et al., Structure-Based Drug Design Strategies and Challenges. Curr Top Med Chem, 2018. 18(12): p. 998-1006.
25. Forli, S., et al., Computational protein-ligand docking and virtual drug screening with the AutoDock suite. Nat Protoc, 2016. 11(5): p. 905-19.
26. Egloff, M.P., et al., The 2.46 A resolution structure of the pancreatic lipase-colipase complex inhibited by a C11 alkyl phosphonate. Biochemistry, 1995. 34(9): p. 2751-62.
27. Morris, G.M., et al., AutoDock4 and AutoDockTools4: Automated docking with selective receptor flexibility. J Comput Chem, 2009. 30(16): p. 2785-91.
28. Sanner, M.F., Python: a programming language for software integration and development. J Mol Graph Model, 1999. 17(1): p. 57-61.
29. Olsson, M.H., et al., PROPKA3: Consistent Treatment of Internal and Surface Residues in Empirical pKa Predictions. J Chem Theory Comput, 2011. 7(2): p. 525-37.
30. Bursulaya, B.D., et al., Comparative study of several algorithms for flexible ligand docking. J Comput Aided Mol Des, 2003. 17(11): p. 755-63.
31. Scarpino, A., G.G. Ferenczy, and G.M. Keserű, Comparative Evaluation of Covalent Docking Tools. J Chem Inf Model, 2018. 58(7): p. 1441-1458.
32. Guerciolini, R., Mode of action of orlistat. Int J Obes Relat Metab Disord, 1997. 21 Suppl 3: p. S12-23.
33. Khedidja, B. and L. Abderrahman, Selection of orlistat as a potential inhibitor for lipase from Candida species. Bioinformation, 2011. 7(3): p. 125-9.
34. Veeramachaneni, G.K., et al., High-throughput virtual screening with e-pharmacophore and molecular simulations study in the designing of pancreatic lipase inhibitors. Drug Des Devel Ther, 2015. 9: p. 4397-412.
35. Roowi, S. and A. Crozier, Flavonoids in tropical citrus species. J Agric Food Chem, 2011. 59(22): p. 12217-25.
36. Zhang, M., et al., Comparison of flavonoid compounds in the flavedo and juice of two pummelo cultivars (Citrus grandis L. Osbeck) from different cultivation regions in China. Molecules, 2014. 19(11): p. 17314-28.
37. Lee, E.M., et al., Pancreatic lipase inhibition by C-glycosidic flavones Isolated from Eremochloa ophiuroides. Molecules, 2010. 15(11): p. 8251-9.
38. Bhattacharjee, B. and J. Chatterjee, Identification of proapoptopic, anti-inflammatory, anti-proliferative, anti-invasive and anti-angiogenic targets of essential oils in cardamom by dual reverse virtual screening and binding pose analysis. Asian Pac J Cancer Prev, 2013. 14(6): p. 3735-42.
39. Venturini, N., et al., Volatile and Flavonoid Composition of the Peel of Citrus medica L. var. Corsican Fruit for Quality Assessment of Its Liqueur. Food Technol Biotechnol, 2014. 52(4): p. 403-410.
40. Jantan, I., et al., Chemical Composition of Some Citrus Oils from Malaysia. Journal of Essential Oil Research, 1996. 8(6): p. 627-632.
41. Furukawa, Y., et al., Isolation and characterization of activators of ERK/MAPK from citrus plants. Int J Mol Sci, 2012. 13(2): p. 1832-1845.
42. Butryee, C., P. Sungpuag, and C. Chitchumroonchokchai, Effect of processing on the flavonoid content and antioxidant capacity of Citrus hystrix leaf. Int J Food Sci Nutr, 2009. 60 Suppl 2: p. 162-74.
43. Loizzo, M.R., et al., Evaluation of *Citrus aurantifolia* peel and leaves extracts for their chemical composition, antioxidant and anti-cholinesterase activities. J Sci Food Agric, 2012. 92(15): p. 2960-7.
44. Chinapongtitiwat, V., et al., Important flavonoids and limonin in selected Thai citrus residues. Journal of Functional Foods, 2013. 5(3): p. 1151-1158.
45. Patil, J.R., et al., Characterization of *Citrus aurantifolia* bioactive compounds and their inhibition of human pancreatic cancer cells through apoptosis. Microchemical Journal, 2010. 94(2): p. 108-117.
46. Spadaro, F., et al., Volatile composition and biological activity of key lime *Citrus aurantifolia* essential oil. Nat Prod Commun, 2012. 7(11): p. 1523-6.
47. Kawaii, S., et al., Quantitative study of flavonoids in leaves of citrus plants. J Agric Food Chem, 2000. 48(9): p. 3865-71.